

Multi-hop Multi-band Intelligent Relay-Based Architecture for LTE-Advanced Multi-hop Wireless Cellular Networks

Hrishikesh Venkataraman · Dipesh Gandhi ·
Vikrant Tomar

© Springer Science+Business Media New York 2013

Abstract In recent years, the cellular spectrum has become very crowded due to the tremendous success of mobile communications. However, a large portion of the electromagnetic spectrum assigned to other services is used sporadically only. A first step towards cognitive radio can be implemented in LTE-advanced networks by sensing the available frequencies and exploiting the existing radio spectrum opportunistically in order to improve its utilization. In this paper, novel multi-hop multi-band intelligent (MMI) radio architecture is proposed for LTE-advanced cellular networks that would make use of a number of intelligent gateways in order to enable simultaneous usage of spectrum resources within the same cell. It relies on a multi-band network model with increasing number of channels which exponentially reduces the time required for resource allocation. Importantly, an analytical model has been proposed to describe the effects of fading on optimum position of gateway. This model was found to have a very close match with the simulation results, in the calculation of mean, standard deviation and the statistically carried out t tests. Further, the two-hop architecture provides a significant increase in the system capacity. With nine bands and 50 nodes in the network, the MMI based two-hop design provides up to 150 % higher than that offered by a single-hop cellular design and with up to 40 % higher than when a state-of-the-art two-hop routing technique is employed.

Keywords Frequency reuse · LTE-advanced · Multi-band · Multi-hop · Spectrum sensing

H. Venkataraman (✉)
School of Electronic Engineering, The RINCE Institute, Dublin City University (DCU), S333,
Glasnevin, Dublin 9, Ireland
e-mail: hrishikesh@eeng.dcu.ie

D. Gandhi
ST Microelectronics, Noida, India

V. Tomar
Telecom and Signal Processing Laboratory, McGill University, Montreal, QC, Canada

1 Introduction

In the last few years, wireless communication systems have experienced a rapid evolution. Now-a-days mobile phones are widely used for various applications and have become much more sophisticated. At the same time, the demand for more bandwidth and higher data rates are increasing at a phenomenal rate. It is anticipated that next Generation (xG) cellular networks would support richer and more diverse services, including VoIP, mobile Internet, video conferencing and mobile gaming, which require increased data rates, even up to 1 Gbps [1]. However, the current cellular networks, such as Global System for Mobile/Wideband Code-Division Multiple Access (GSM/WCDMA) and Wireless interoperability for Microwave Access (WiMAX) networks, can support data rates of up to 100 Mbps only. In addition, they may not be economically feasible to cater to the higher data-rates and strict Quality of Service (QoS) requirements of future mobile communication services [2]. Hence, it is questionable whether the next generation systems would be able to cope with the increasing spectrum demands even with their evolved transmission techniques. In order to satisfy the growing demands, there is a need to conceive new and more efficient ways to utilize the available limited spectral resources [3]. In November 2002, the Federal Communications Commission (FCC), US published a report aimed at improving the way in which the radio electromagnetic spectrum is managed in US [4]. This report noted that some frequency bands in the radio spectrum, especially the mobile bands, are heavily occupied most of the time, whereas, other frequency bands are only partially occupied or largely unoccupied (e.g. TV bands). These fragmented frequency bands which are not used by the licensed user at any given time and a specific geographic location are known as *spectrum holes*. Cognitive Radio (CR) has been proposed as means to promote efficient use of the spectrum by exploiting the existence of spectrum holes. The CR principle is to utilize opportunistically various spectrum holes eventually hopping from one to another, so as not to affect the primary user activity [5,6]. A first step towards cognitive radio would be to dynamically re-farm the available frequencies in order to efficiently utilize the available frequency resource.

Figure 1 shows a possible and most probable next generation long-term evolution-advanced (LTE-advanced) cellular network architecture. It consists of the base station (BS) at the centre of the cell, mobile stations (MSs) and relays that not only serve as repeaters/access-points, but also act as cognitive devices capable of sensing the available spectrum in the environment [7]. All the wireless devices in the network communicate with other devices in their neighbourhood, and also with the relays/cognitive gateways (CGs). This paper presents a new multi-hop multi-band intelligent relay architecture (MMI) which enhances the spectral efficiency and the overall performance of existing cellular networks by making use of a number of CGs. Using the MMI architecture, the time required for resource allocation and notably, the time delay before channel allocation, even under high traffic conditions, is significantly decreased. The novelty of the MMI architecture lies in an efficient design for spectrum sensing and spectrum sharing in cellular networks. A detailed mathematical analysis is carried out in order to determine the number of CGs that would maximize the carrier to interference ratio, γ , of the communicating receivers. In addition, the time required for resource allocation and the Shannon capacity of the MMI-based cellular network is compared against a single-hop cellular architecture and state-of-the-art two-hop design.

Section 2 discusses the motivation and the related work. Section 3 describes the proposed MMI system architecture. Section 4 presents the simulation set up and Sect. 5 discusses the performance of the MMI architecture in terms of the required time and the system capacity. Finally, Sect. 6 concludes the paper.

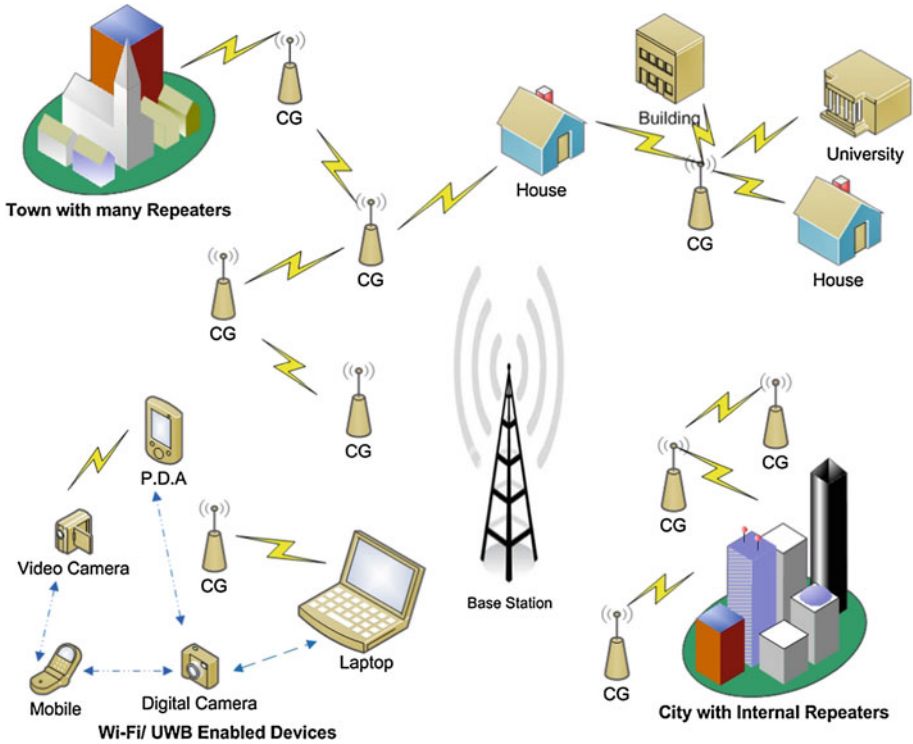


Fig. 1 Next generation multi-hop cellular network with cognitive gateways

2 Related Work

There have been significant works on micro-cell approaches, coding techniques and channel allocation solutions for various traffic types in cellular networks [8,9]. Different techniques include channel-borrowing algorithms and fault-tolerant channel assignment solutions that have been developed to improve the performance of cellular networks. However, these works were based on a definite set of frequencies (channel resource) and are not in synchronization with today’s demand for high-rate data-centric communications. Moreover, these algorithms did not utilize the unused spectrum from the neighbouring bands.

2.1 Cognitive Radio

CR-based next generation wireless networks are very promising, yet are relatively very complex. This is because; they involve spectrum sensing, spectrum sharing and dynamic spectrum management. Additionally, there are also non-trivial issues such as interference avoidance, traffic allocation, frequency shifting, synchronization, etc. [10]. In terms of spectrum sensing, there are three different methods for signal detection. The most common method is the *matched filter* technique, which is an optimal way for any signal detection. However, its main drawback is that it requires effective signal demodulation and hence, requires a priori knowledge of the signal at both PHY and MAC layers. A second method is based on *energy detection*, basically a non-coherent detection method. However, energy detector has several drawbacks like susceptibility to changing noise levels, limitations in detecting spread

spectrum signals, etc. that hinders its use [9]. The third method of spectrum sensing is the *cyclo-stationary solution*. This is found to be significantly superior and hence, is normally the most preferred spectrum sensing technique [11]. Notably, there have been improvements to the classic cyclo-stationary detection to sense spectrum holes [12,13]. Kim et al. [14] proposed an OFDM based system architecture for CR networks which uses adaptive traffic allocation in time and frequency to minimize the interferences with the primary users. Similarly, Arslan et al. [15] proposed an interference avoidance algorithm for OFDM-based cognitive radio on reconfigurable architecture while Michalke et al. worked on the idea of using MIMO-OFDM technique in the systems [16,17]. On the other hand, Weiss and Jondral [18] addressed the signalling and synchronization issues for spectrum pooling.

Importantly, there are still two major problems that hinder the development of new and highly efficient CR-based wireless systems. Firstly, the demand of adopting an entirely new architecture would result in overhauling the entire network design, which in turn would require huge investments. This is not feasible from either practical or financial reasons [19]. Secondly, there is a need to process multi gigahertz (GHz) wide bandwidth and reliably detect the presence of primary users over a wide-band spanning a couple of gigahertz. Currently, the mobile devices work on dual/tri/quad bands (900, 1,800 MHz ranges, etc). However, communication over a frequency spectrum spanning 2–3 GHz has not yet been achieved [20]. In order to overcome these challenges, this paper proposes to enhance the existing cellular network architecture with CR, multi-hop and multi-band features.

2.2 Multi-hop and Relays

Multi-hop cellular networks are an active area of interest. The multi-hop cellular architecture offers many advantages, such as increased network throughput, scalability and coverage [21,22]. To maintain a specific link quality, the required transmit power of the communicating link should increase with an increase in the data rate. Providing very high data rate services in the future will either require high transmission power or shorter transmission distance between the communicating links. One simple way is to increase the density of cells/BSs (i.e., smaller cells and higher number of BSs would satisfy the increasing data rate demand). However, increasing the number of BSs increases the system cost substantially [23], which is not desired. A multihop system solves these power limitations by using relay nodes without demanding any significant change in the existing infrastructure [24]. This in turn ensures that the system cost does not increase considerably. In addition, applying relaying in an infrastructure-based network obviates the necessity for complicated distributed routing algorithms as compared to *ad-hoc* networks [25].

Considerable work has been done in the two-hop network domain. The authors [26] presented a mechanism for increasing the system capacity in a two-hop network. Further, the best path for relay selection and its implication on the system capacity was analyzed in [27,28]. However the researchers did not identify the mechanism for finding the best path under different conditions. Further, Huang et. al. presented a design mechanism that showed the optimum relay location for specific two-hop wireless network [29]. A major drawback of the current literature on two-hop networks and in general, multi-hop networks is that they still have not resulted in compelling amount of intelligence to the relays.

2.3 CR, Multi-hop and Multi-band

IEEE 802.22 defines the air interface based on CR techniques for the opportunistic use of TV bands on a non-interfering basis. In the 802.22 standards, the cognitive radio is placed in

the end-user device, which sends feedback messages to the BS. There is no multi-hopping in the current IEEE 802.22, unlike the multihop based IEEE 802.16j networks. However, it is important to understand the core differences between 802.22 and 802.16 (WiMAX). 802.22 mostly targets rural and remote areas, and currently investigate the communication mechanism over a single-hop network only, not defining multi-hop. However, there have been several works in the recent past [30,31] that investigate multi-hop in CR networks. In fact, the author in [32] pointed out that multi-hopping significantly improves the performance of CR-based networks. Complimentarily, there exist tri-band and quad-band mobile phones in the market [33,34]. However, considering the next generation networks, designing solutions which scan the entire width of the spectrum (for example, from 800 MHz to 2.4 GHz) is an extremely challenging task [35]. In addition, the size and power requirements of the local oscillator increase with an increase in the oscillating frequency range, thereby making it *unsuitable* for portable mobile devices. This calls for a multi-band design in the next generation cellular networks. The next section describes the network architecture of multi-hop multi-band design in detail, along with the importance and benefits of having relays as intelligent nodes.

3 MMI Network Architecture

The MMI network architecture proposed in this paper consists of two different phases: spectrum sensing and frequency hopping, to sense the spectrum holes and change the transmission and reception frequency respectively. This approach only requires installation of cognitive gateways (CG) within the existing cellular infrastructure. All the communications is routed through the CG's which can be done using software, and hence, does not have a high cost of implementation. The detailed explanation is provided as follows:

3.1 Architecture Overview

The MMI architecture is composed of BSs, CGs and MSs. This paper focuses on a two-hop based MMI system design; though the design would be extended to higher hops, particularly, for three-hops in future. A single-cell representation of a MMI based system is shown in

Fig. 2 Multi-cluster architecture with all CGs in the cell located at equidistant distance from the BS

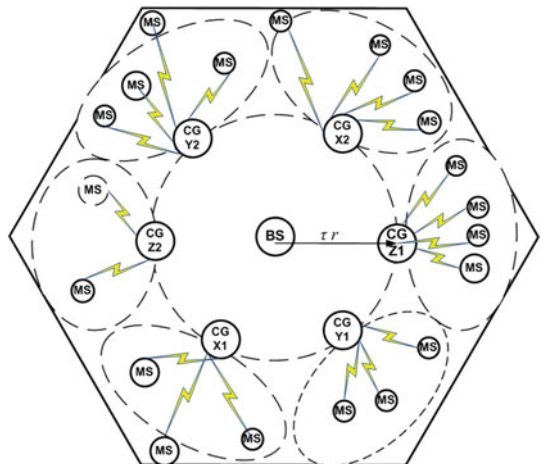


Fig. 2. The MMI architecture follows from a cluster-based design that was proposed for two-hop cellular networks [26, 36, 37]. Each hexagonal cell in the cellular network is divided into two regions: the *inner region* and the *outer region*. In the inner region, the BS communicates with MSs directly if there is a radio resource (time instant in case of time division multiple access/frequency resource in case of frequency division multiple access) available, whereas in the outer layer, the BS always communicates with MSs through CG. Each hexagonal cell has an edge length, r , and the inner region has a radius, τr . Here, τ represents the ratio of the distance of the inner layer to the length of the cell edge; and is given by $0 \leq \tau \leq 1$. The CG's are equidistantly placed and are located at a distance of τr from the BS. In any and every time instant, there are two simultaneously communicating pairs, located within diametrically opposite clusters with respect to the BS. Further, in the adjacent time instants, two diametrically opposite pairs from other CGs communicate simultaneously. Hence, in a time division based MMI network, communication over a CG occurs only in bursts for only a small fraction of time and not continuously for the entire time frame. Moreover, if the CG is not able to forward the data in that particular time slot, it would store that information in its buffer before forwarding it further in the next time slot. Further, in a multi-cellular scenario, each cell is surrounded by 6 cells in the first tier and 12 cells in the second tier. In addition, the same resource is used by two simultaneously communicating pairs in every adjacent cell in the 7-cell scenario. Hence, a frequency reuse ratio of *one* is achieved. Importantly, every cell in the network is assumed to have a primary user. This implies 19-cell architecture with 19 primary users in a 19-cell network. Hence, the primary user in every cell would experience interference from other primary users. In addition, there could be a second user in the cell (secondary user) depending on factors like: whether the primary user is communicating, the amount of interference created by the secondary user to the primary user, etc. This second user in every cell is located diametrically opposite to the primary user. In case of a communication from BS to CG (say CG X1, as illustrated in Fig. 2) as the primary communicating pair, the secondary pair could be communicating from a CG (say CG X2) that is located diametrically opposite to CG1, to the end users (mobile nodes) in that neighbourhood. An early form of this design has been investigated for a non CR network in [26].

It should be noted that having diametrically opposite CGs ensures that the CGs are spaced maximum distance apart in the cell and hence would cause minimal interference to each other. At this stage, it should be noted that the most important source of interference is the co-channel interference (interference arising from re-use of the same channel). The adjacent channel interference (if any) is neglected in this work. Further, since a CG communicates with several MSs, the CG will definitely communicate over the same time period when the BS communicates with the diametrically opposite CG. However, the MMI architecture does allow communication across non-diametrically opposite clusters. In case the diametrically opposite CG does not have any traffic to send, then there are two options that are considered in the design:

- i. A non-diametrically opposite CG is selected for transmission, according to the amount of backlog traffic from previous time slot. This reduces the distance between the simultaneously communicating pairs which in turn increases the overall interference, depending on the exact location of the simultaneously communicating interferers.
- ii. If no CG has any back-log traffic (or if the additional interference is too high), then no secondary pair communication takes place over that small time period in that cell.

Hence, on a whole, the diametrically opposite CGs is the preferred mechanism in the MMI architecture. Importantly, this arrangement (of having CGs diametrically opposite to the BS) ensures that there is a certain minimum distance between the primary and the secondary users

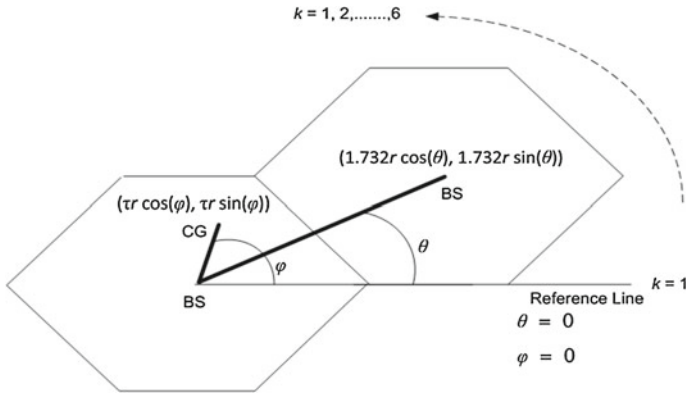


Fig. 3 Calculation of distances (and angles) between the communicating pairs in adjacent cells

which would inherently avoid the hidden node problem in the CR network. Notably, it should be noted that the number of CGs in a cell could be increased beyond two, but should be an even number (four, six, etc.), thereby having diametrically opposite CGs. This is especially beneficial in case of high traffic load in the system, where equidistant CGs would distribute the traffic load among them in an almost equal manner. This in-turn would result in reduced power requirement and time required for resource allocation.

3.2 Role of CG in the MMI Architecture

Any CG has two fold functionality:

- i. Acts as a cognitive radio and senses the spectrum holes, and
- ii. Serves as a fixed relay, i.e. receives and passes-on the signal to/from the BS, neighbouring CG's or the mobile receivers.

For the MSs located in the outer region of the cell, the CGs in the MMI architecture also act as relays/heads of a *constellation*. A typical constellation could be represented with an elliptical shape as shown in Fig. 2. The MSs in each of the constellations communicate with the BS through their constellation-heads/CGs. Also, as can be seen from Fig. 2, there is a small area between two elliptical clusters. The MSs in these areas are assigned to one of the clusters. The constellation could however be still approximated by an ellipse [36]. As shown in Fig. 3, every point in the elliptical constellation region is uniquely determined by the vector: $\beta (a \cos \theta_i + b \sin \theta_j)$, where $0 \leq \theta_i < 2\pi$ is the angle measured from the centre of the ellipse to the position of the MS [37]. By varying the value of β from 0 to 1, the whole area of the ellipse is spanned, with b and a being the semi-major axis and semi-minor axis of the ellipse, respectively. It should be noted that placing the CG at the circumference of the ellipse at the edge of the minor-axis is a very practical approach. This enables having a $2\pi/3$ directional antenna at the CG that would cover the entire region of the ellipse and results in effectively communicating with all the MSs in that cluster.

3.2.1 CGs in Multi-hop Architecture

An intelligent placement of CGs provides significant benefits. Firstly, the CGs act as relays between BS and mobile nodes. This in-turn results in a reduction in the effective transmission

distance of a communicating pair thereby reducing the required transmitted power. Theoretically, the CGs could be placed at the BS itself. But, from the perspective of the radio network design, this placement would result in an inefficient design. Since the CGs take spectrum from different sources like TV station, radio station, other cellular operators, having CG at the BS of a multi-hop cellular network results in an additional infrastructure requirement of having both a CG and a relay. Even if no multi-hop transmission is considered, having a CG at the BS itself implies that the receiver sensitivity of the CGs have to be much higher due to the increased transmission distance between the mobile node and the CG. In addition, if there is no multi-hop, the CG would not have the flexibility of assigning the same frequency resource to different users in the adjacent cells. Last but not the least, placing a CG at sources like TV station, radio tower, etc. for commercial civilian applications would require considerable bureaucratic permissions and might not be feasible. Hence, in the multi-hop multi-band cellular design, the location of CG is considered to be different than the position of the BS.

3.2.2 CGs in Multi-band Architecture

The problem of processing multi-gigahertz wide bandwidth can be addressed by dividing the entire band into a number of smaller bands distributed discretely in the entire spectrum. Each of the sub-bands could have equal width. For example, if 25 MHz sub-bands for either uplink or downlink are considered, and the total spectrum of operation ranges from 800 MHz to 2.4 GHz, then the number of sub-bands to be used for communication, including uplink and downlink, is 32. Considering the rapidly evolving VLSI and nano-electronic technologies, and the shrinking size of the chips and transistors, accommodating several small local oscillators on a next generation mobile device, each of which scanning a small narrow-band spectrum, seems to be very much achievable.

In the MMI design, each CG consists of several local oscillators. Any local oscillator in the CG senses the spectrum in the aforementioned finite bands and not the entire width of the spectrum, and changes the transmitting/receiving frequency to one of the free bands as and when required. The resulting change in the frequency band is indicated by the CG to the mobile node, prior to the transmission of next data packet. The multi-band model is independent of the multiplexing technique and hence, would work equally well with both time division duplexing (TDD) and frequency division duplexing (FDD) modes. The end user mobile devices would not sense the network; hence need not be modified. This is a significant advantage of this design—it *does not ask for change in the end-user's handsets*. Importantly, this reduces the cost of the end-user device. At the same time, the mobile device would be a multi-band terminal, and would be able to switch between the different bands as and when signalled by the CG. With the advancements in digital signal processing technology, multi-band switching is not only feasible, but also a very realistic solution towards realization of next generation wireless devices. The different functionality of the MMI system architecture that enables the sharing of electromagnetic radio spectrum is explained in the next section.

3.3 MMI Network Functionality

The functionality of the MMI system can be explained by considering a downlink transmission. The BS communicates with all the CGs in its cell by broadcasting a start signal. On receiving the start signal, all CGs start to sense the spectrum for vacant spectrum bands (i.e., spectrum holes). The CG nearest to the BS sends the sensed spectrum data to the BS/wireless node informing it about the available bands to communicate. The range of transmission of a CG is limited to the first tier only and it acts as a relay between:

- i. BS and the mobile user or another CG,
- ii. Two CGs, or
- iii. Another CG and the mobile receiver.

Each CG maintains a table, referred to as spectrum table. The CG senses the spectrum by using the cyclo-stationary detection method as explained in [11]. As soon as a CG senses the primary user in a vacant band, it adds this band in its table and broadcasts this information to its first-tier-neighbourhood CGs. If a CG/any wireless node is transmitting and the primary user of that particular spectrum decides to transmit during that period, the CG would sense the primary user and immediately stop transmitting (or ask the wireless node to stop transmitting) in that band. In addition, at the next time instant, the CG switches its transmission to the nearest vacant band. It then broadcasts a beacon or frequency tone to indicate the occupancy of the band over which it is going to communicate. The CGs continue to sense the spectrum and the updated table are synchronized periodically after every finite interval. In a UMTS system, as considered in our analysis further, this interval is kept at one UMTS frame, which is 10 ms long. It should be noted that one UMTS frame has 15 time slots. Hence, for three pairs of CGs in the architecture, each diametrically opposite pair of CG would communicate for 5 time slots each. This synchronization is done primarily so that all the adjacent CGs are aware of various available or in-use spectrum bands. This would serve as a useful reference while allocating spectrum bands to the incoming users/mobile nodes. It should be noted that the interval of 1 UMTS frame is decided based on the current standard. Several UMTS frames could also be considered together, according to the specifications of a particular standard. However, the overall mechanism for transmission still remains the same.

In the proposed design, there is always one primary user per cell BS \rightarrow CG in case of downlink and CG \rightarrow BS in case of uplink; and a maximum of one secondary user per cell CG \rightarrow MS in case of downlink and MS \rightarrow CG in case of uplink. Further, given the hierarchical nature of the two-hop communication model in the MMI architecture, the secondary communicating pair in the design has a relatively steady position where the position of CG is fixed and the MSs are located within the elliptical cluster. A TDD/TDMA UMTS-based design is considered for the physical and MAC layer modelling. The relevant parameter selection in the implementation aspect is explained in Sect. 4.

The architecture is developed in order to achieve a frequency reuse of one (i.e., a pair communicating continuously in every cell, or two pairs communicating over half the time period each). In a scenario with the centre cell, first tier of 6 adjacent cells and the second tier of 12 cells; there would be at least 19 simultaneously communicating pairs (one in the centre cell+ six in the first tier and 12 in the second tier). Considering that there could be one secondary user per cell, the total number of communicating pairs (including primary and secondary) is 38. Hence, the number of communicating pairs in a 19-cell network varies between 19 and 38; i.e., $19 \leq n_t \leq 38$. Given a multi-hop scenario, a slow varying frequency flat fading channel is considered in the design. Hence, if P_T is the transmitting power and d_c is the transmission distance of the desired communicating pair expressed in meters, the received power, P_R could be written as given in Eq. (1) and [38,39]:

$$P_R = P_T - (k_1 + 10\alpha \log_{10}(d_c) + \zeta) \quad (1)$$

where k_1 is the propagation constant, α is the path-loss exponent and ζ is the lognormal shadowing component. ζ is a random variable and is independent of the distance between the transmitter and receiver. If there are n_t simultaneously communicating pairs in the network that utilize the same radio resource at any time instant, t , then the receiver in each of the n_t communicating pairs would experience interference from $n_t - 1$ transmitters. Each primary

user creates interference with both other primary users and any secondary users in the network. In the wireless network design, the amount of interference determines the capacity of the network, the number of simultaneous communication, the amount of resource reuse and importantly, the time required for establishing end-to-end communication. Hence, interference calculation is an integral part for finding the system capacity of the network. Further, the exact amount of interference depends on the number of total communicating pairs, the distance between the different interfering users, the power transmitted by the interfering signals and the power dissipation rate of the communicating link.

3.3.1 Interference and Capacity Calculation

In the initial part of the analysis, the lognormal shadowing factor ζ is taken as zero. For such a scenario, the received power and the interference is solely a function of the distance. Figure 3 shows the k cells in the first tier and the distance of the interfering transmitter from the neighbouring cell to the centre cell. Here $p = 1.732$ and τ represents the fraction of the cell radius that lies in the inner region. θ_k represents the angle θ for the k th cell that is located in the first tier. The total number of interfering cells for any receiver in the centre cell is however from both the first and second tiers, represented by i number of cells. Hence, the angle is represented as θ_i , for $1 \leq i \leq 19$. Considering this, the γ experienced by the receiver of a communicating pair is given as:

$$\gamma = (d_c)^{-\alpha} / \sum_{i=1}^{n_t-1} (d_{inti})^{-\alpha} \tag{2}$$

In the above equation, α represents the path-loss exponent of the communicating link, i represents the current communicating pair and is given by $i \in \{1, \dots, n_t\}$, wherein n_t represent the total number of communication pairs (including both primary and secondary pairs). The Shannon capacity of the network at any time instant (in bps/Hz) is given as:

$$C = \sum_{i=1}^{n_t} \log_2(1 + \gamma_i) \text{ bps/Hz} \tag{3}$$

As is evident, the Shannon capacity calculated per Hertz is dependent only on γ . Therefore, the behaviour of Shannon capacity is the same as that of γ .

3.3.2 Path-Loss Based Interference and γ Calculation

In a real-world scenario, there always exists some amount of shadowing. This is accounted by the shadowing factor, ζ . The effect of this lognormal shadowing on the MMI architecture can be computed by defining an additional distance, d_ζ between the transmitter and receiver arising due to this shadowing. Hence, for the desired transmission pair, relationship between ζ_c and d_ζ could be written as $\zeta_c = 10\alpha \log_{10}(d_\zeta)$. Therefore, for the desired transmitter-receiver pair, the lognormal shadowing could be represented by the equivalent distance as $d_\zeta = e^{0.1\zeta_c/\alpha}$. Hence, the carrier-to-interference ratio in the presence of shadowing is given by:

$$\gamma = (d_{c \times d_{\zeta c}})^{-\alpha} / \left(\sum_{i=1}^{n_t-1} (d_{inti} \times d_{\zeta i})^{-\alpha} \right) \tag{4}$$

where $d_{\zeta C}$ and $d_{\zeta i}$ are the additional (virtual) distances which take into account the effect of log-normal shadowing. In the absence of any shadowing, $d_{\zeta C}$ and $d_{\zeta i}$ values are zero. This is a well-studied problem and in fact, it has been shown in [35] that in the absence of any shadowing, the optimum locations of φ that maximizes γ are: $\pi/3, 2\pi/3, \pi, 4\pi/3, 5\pi/3$ and 2π . However, in the presence of shadowing, there is a significant effect of the additional distance accounted due to the log-normal shadowing, as can be observed from Eq. (4). In order to find the angle φ that results in optimum system capacity in the network in the presence of shadowing, the derivative should be zero and the double derivative should be negative. For that, Eq. (4) is differentiated with respect to φ , resulting in Eqs. (5) and (6).

$$D(\gamma) = 1.732\alpha\tau^{(1-\alpha)r(2-\alpha)} \times \left(\sum (d_{int i} \times d_{\zeta int i})^{-(\alpha+2)} \sin(\varphi - \theta_i) / \sum (d_{int i} \times d_{\zeta int i})^{-\alpha} \right)^2 \tag{5}$$

and

$$D^2(\gamma) = \frac{P1 \times \left(\sum (d_{int i} \times d_{\zeta int i})^{-(\alpha+2)} \sin(\varphi - \theta_i) \right)^2}{\left(\sum d_{int i} \right)^2} - \frac{P2 \times \sum (d_{int i} \times d_{\zeta int i})^{-(\alpha+4)} \sin^2(\varphi - \theta_i)}{\left(\sum d_{int i} \right)^2} + \frac{P3 \times \sum (d_{int i} \times d_{\zeta int i})^{-(\alpha+2)} \cos(\varphi - \theta_i)}{\left(\sum d_{int i} \right)^2} \tag{6}$$

where $D(\gamma) = d(\gamma)/d(\varphi)$

$$D^2(\gamma) = d^2(\gamma)/d(\varphi)^2$$

$$P1 = 1.732\alpha\tau^{1-\alpha} (d_{c_x}d_{\zeta c})^{2-\alpha} \times 2\sqrt{3}\alpha\tau (d_{c_x}d_{\zeta c})^2$$

$$P2 = 1.732\alpha\tau^{1-\alpha} (d_{c_x}d_{\zeta c})^{2-\alpha} \times (\alpha + 2)\sqrt{3}\tau (d_{c_x}d_{\zeta c})^2$$

$$P3 = 1.732\alpha\tau^{1-\alpha} (d_{c_x}d_{\zeta c})^{2-\alpha}$$

and \sum implies summation from 1 to $n_t - 1$.

Further, since the log-normal shadowing is a continuously variable parameter, it is not possible to determine a fixed optimum value of φ . Hence, we consider a statistical-based analysis to get a more meaningful value for optimum value of φ . The log-normal shadowing considered in this work has zero mean and a standard deviation of 2–6 dB. This in-turn implies that in absolute scale, the standard deviation of log normal shadowing varies from 1.59 to 3.98. Importantly, the shadowing of each of the n_t path (i.e., desired communicating transmitter and receiver and $n_t - 1$ interfering transmitter with the intended receiver) are independent of each other. Hence, applying central limit theorem for large numbers, the sample variation of φ would definitely converges to the expected value as the number of simultaneously communicating pairs approach infinity. Following this approach, the variation of optimum γ with respect to φ follows a Gaussian distribution around the values of $\pi/3, 2\pi/3, \pi, 4\pi/3, 5\pi/3$ and 2π , with a standard deviation (σ_ϕ) equal to:

$$\sigma_{\phi \text{ abs}} = \sigma_{\gamma \text{ abs}} / \sqrt{(10 \times (\alpha - 1) \times (n_t - 1))} \tag{7}$$

where σ_γ is the standard deviation of the log-normal shadowing. Hence, for a two-hop MMI system with interference from intra-cell and two simultaneously communicating pairs across every cell in the first tier, the total number of interferers for every pair would be $n_t - 1 = 13$.

Importantly, for a wireless transmission with a path-loss exponent of $\alpha = 3$, this implies that in the calculation of γ , the standard deviation of γ would be $\sqrt{260}$, i.e., 16.12 times less than the deviation in the signal strength due to a single entity. Therefore, the standard deviation of φ varies from 0.0986 to 0.2468 (in radians). In terms of degrees, the standard deviation of φ therefore varies from 5.655 to 14.12. These statistical results will be compared in detail with the simulation results in Sect. 5.

3.3.3 Variation of Transmission Power

In real-world scenarios, the transmission powers of the CG and the MS changes with time, depending on the radio channel conditions. Changing the transmit power ratio (i.e., the ratio of transmit power of BS and the transmit power of CG) mainly changes the value of τ : i.e., it changes the distance from the BS where the CG should be optimally placed. This would very well converge with the MMI architecture design, as with an increase in the CG transmit power; the CG would be able to transmit to the far-located MSs and could well be placed closer to the BS. It should be noted however, that the transmit power ratio between BS and CG does not affect the optimum number of CGs *six*. This is because; the optimum number of CGs depends mainly on the cell layout and the position of interfering transmitters. As the ratio of the transmitted power between the BS and the CG is varied (keeping the position of CG fixed), the overall system capacity decreases by a small amount. However, it would still be optimal for the given placement of CGs.

4 Simulation Model

A multi-hop cellular network is simulated in Matlab, with communication between BS and MSs in each cell taking place in a maximum of two hops. 5,000 MSs are assumed to be uniformly distributed in 19 cells within a coverage area of 10 km^2 . Consequently, the side of a hexagonal cell (r) would be 62.04 m. The MMI architecture described in Sect. 3 is considered in the system deployment. There are six CGs in every cell that are equidistant from each other and from the BS. The MSs located further from the CG in the cell communicate with the BS through the CG in two hops. Prominently, the CGs act as both relays and multi-band radios. A slow fading Gaussian wireless channel is assumed throughout the study.

A total bandwidth range of 100 MHz is considered in the simulations. Notably, 5 MHz are taken as the band for a unidirectional link. The uplink and downlink scenarios are considered in the simulations separately. Hence, 50 MHz are allocated for uplink and downlink each respectively. Nine bands with 5 MHz each are considered in any direction in the system design. The number of frequency bands in the network is varied from *one to nine*. Of these, one of them is the cellular band, whereas the other *eight* bands actually belong to other unused/scarcely used radio bands like TV, radio, military, etc. This constitutes 45 MHz. The remaining 5 MHz band is used for control signalling only. A UMTS system of channel allocation is considered with channels of 200 KHz and with several time multiplexed users in each channel. This implies that over a band of 5 MHz, there are 25 channels. Hence, over a band of 50 MHz in downlink (or uplink), there are 1,250 channels, of which 1,125 channels are used for communication and other 125 channels for control messages. It should be noted that this channel arrangement is for UMTS based systems and that the remaining 125 channels are used exclusively for control information. The CG considers different unutilized frequency bands for allocating frequency to the communicating links. The frequency of operation of different communicating links is determined by the CG depending on the available frequency resource

in the multi-cellular network. Determining the exact feedback mechanism and exchange of signalling information is out of scope of the current work, and hence is left for further research.

The centre frequency of operation is considered to be around 2 GHz. Hence, for a 100 MHz bandwidth, the frequency under consideration is 1,950–2,050 MHz. The propagation constant can be considered to be almost the same. In the simulations, the propagation constant is taken as $k_1 = 20$. Similarly, a constant path loss exponent of $\alpha = 3$ has been considered in the simulation model. In order to take into account the effects of fading during propagation, a lognormal shadowing with zero mean and standard deviation of 4 dB is considered while calculating the system capacity, based on a realistic semi-outdoor environment. The transmission power of the BS is kept at 1 W, whereas that of the CG is 5 times lower: i.e., 0.2 W. The simulation model calculates the value of γ and the system capacity, C , for seven cells independently (centre cell + six adjacent cells) and then takes an average over these seven cells. The communicating pairs in the twelve cells in the second tier are for the calculation of interference only. In the absence of any existing standard, an UTRA-TDD time frame of 10 ms is considered in the simulations. There are 15 time slots per frame. Each time slot transmits 60 symbols. BPSK (the lowest modulation scheme) is considered for the transmission of packets. Hence, 60 bits are transmitted during one time slot and $60 \times 15 = 900$ bits over a 10 ms frame.

Every wireless device (BS/CG/MS) in the cell has certain traffic to be transmitted to its destination node. The minimum data that a wireless device could transmit can be zero, but the maximum traffic/packet size at any sampling instant is restricted to 100 symbols. The expected number of mobile nodes requesting communication is 1 every minute. The average duration of the connection is considered to be 3 min (180 s). Similarly, the average duration of a particular band used is also 3 min. Since majority of the traffic in the next generation wireless systems is expected to be in the downlink direction, the focus of study in this paper is also for the downlink mode. Further, it should be noted that one of the main purposes of having a CR-based network is to improve the overall system performance. The performance that matters in the next generation Internet-based multimedia-centric wireless world include: *fast access to information* and *getting as much information in a unit of time*. Hence, in this research work, the *time taken for resource allocation* and *system capacity* are considered as metrics for performance assessment.

The CG detects the available frequency resource in its vicinity and allocates it to different communicating links, for which the CG needs some definite time interval. Hence, in a multi-band network, there is some delay in establishing communication across the communicating links in the system. The total time delay, T_d before the start of the communication is composed of:

- i. The sensing time, T_s ,
- ii. The time for resource allocation, T_r and
- iii. The time for setting up the connection, T_C .

Therefore, the total time delay is expressed in Eq. (8) as:

$$T_d = T_s + T_r + T_C \quad (8)$$

Of these, the time required for resource allocation, T_r is the lowest and importantly, has a near constant value. The time required for setting up the connection, T_C , depends on the availability of resources. If there are very few resources to be used by several users, then the time required for actually setting up the connection, T_C is quite high. If the number of unutilized channels is low, then the multi-band architecture requires more setting up time as the same number of channels have to be reused by many communicating pairs.

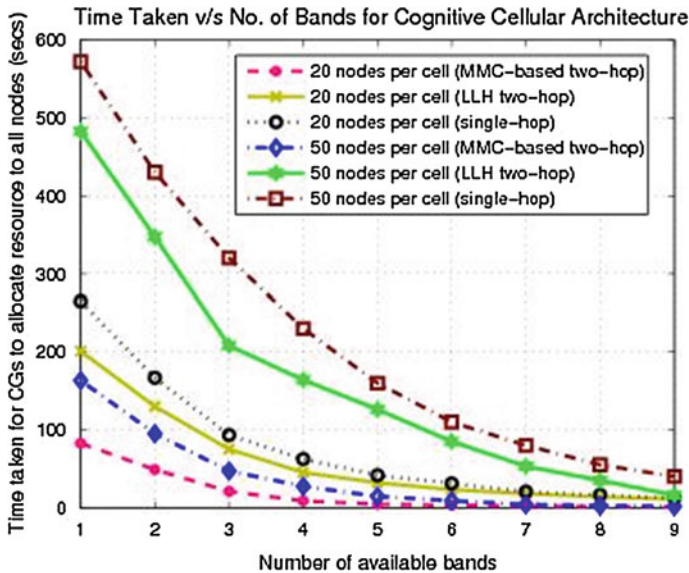


Fig. 4 Variation of time delay with number of frequency bands (less than 100 nodes per cell)

However, as the number of channels that could be detected and assigned is increased, the CG has additional resources to allocated to the multihop links. This in-turn not only reduces the time required for all the links in the system to communicate, but also reduces the number of times, a particular resource is to be reused. Notably, another important component with regard to time delay is the time required for sensing the availability of radio resource, T_s . The time required for sensing varies from just a few milli-seconds to couple of seconds, depending on the amount of frequency band the CG has to scan before finding an available frequency band for communication. It would be interesting to observe that a CR network with access to different unused spectrum bands can significantly reduce the time required for communication which would be extremely beneficial in a high traffic scenario.

The next section illustrates the benefits in terms of the time reduction in the resource allocation and the improvement in the system capacity, as compared to single-hop cellular network and a least longest hop (LLH)-based two-hop cellular network. The LLH method was one of the three state-of-the-art methods proposed and investigated for relay-based cellular networks [39,40]. In fact, it has been demonstrated for a non-CR network, the LLH scheme provides much improved performance over other two methods—shortest total distance (STD) and shortest relay hop distance (SRD) [26].

5 Performance Results

5.1 Time Delay in Resource Allocation

Figure 4 presents the time taken for CGs to allocate resources to all the nodes versus the number of available channels. It can be observed from Fig. 4 that there is an exponential decrease in the time required for both one-hop and two-hop transmission, when the number of channels that could be assigned by the CG increases. The time required in the MMI

architecture is due to the time taken by the CG to allocate the resources, and by the wireless node to get the assigned frequency resource. In a MMI-based two-hop transmission, the time required is 8.72 s when there are 20 nodes per cell and there are only 4 available bands (or 100 channels) in the system. However, when the number of bands is increased to 8 (200 channels), the total time taken reduces to 1.12 s. It can be noted that the time required for resource allocation reduces exponentially with an increase in the number of channels.

In addition, it can be seen from Fig. 4 that the time required for a multi-hop multi-band architecture is much lower than that of a single-hop or LLH method. For example, for 50 nodes/cell with 8 bands allocated to one cell, the time required in case of single-hop and LLH-based two-hop network is 55 and 35 s respectively whereas the time taken for MMI-based architecture is 2.62 s,—*13 times less than the measured value when LLH routing method was used; and 21 times less as compared to the single-hop design*. It should be noted that this time reduction in the LLH and MMI two-hop design does not take into account the marginal increase due to the additional overhead in a two-hop network. However, the overhead delay is usually in the order of few milliseconds. Hence, it is expected that, even after considering overhead, the time taken by the two-hop design is much lower than that of the single-hop network model. An important aspect of the MMI architecture is that it is scalable with the increase in the number of nodes in the cellular network. This is unlike the simple multi-hop architecture wherein, in the absence of a multi-band design, the existing scheduling techniques are unscalable. Also, the time delay rises beyond the acceptable margin. However, Fig. 5 shows that the MMI architecture is scalable even when the number of communicating nodes in each cell is increased beyond 100. It can be observed from Figs. 4, 5 and Table 1 (*italics for MMI measurements and bold for LLH measurements*) that with an increase in the resources, the time required for the multi-band network decreases at a similar rate for both higher and lower number of nodes in the network. For example, in case of 250 nodes, the time required for MMI architecture reduces from 950 to 337 s when the number of channel is increased from one to three, i.e., a reduction of nearly 66%. Similarly, when the number of nodes is 50, the time required form MMI architecture when the number of channels is one and three are 172 and 51 s respectively, again a reduction of nearly 66%. This is a very important result. It signifies that in order to reduce the total time delay, the CG should have certain number of unutilized frequency resources which it can assign to the communicating nodes, in order to ensure that the time taken for resource assignment is within few seconds.

5.2 Improvement in System Capacity

The performance of the multi-band architecture is analyzed by simulating the packet transmission in the network in the downlink mode. The system capacity of the two-hop cellular network is measured with regard to different number of available channels. In the simulations, the system capacity is calculated for the centre cell and the first tier of six cells only. The traffic in the second tier of twelve cells is used mainly for calculating the interference in the first tier of six cells. Figure 6 shows the system capacity when there are 50 nodes/cell. It can be seen from Fig. 6 that in the presence of only one channel, the median of CDF for 50 nodes/cell is 1.43 bps/Hz/cell whereas in the presence of all 9 bands, the median is 2.52 bps/Hz/cell: i.e., an increase of 76%. In order to determine the improvement in terms of the system capacity, the two-hop multi-band architecture is compared with the single-hop design and with the least longest hop (LLH) routing model designed specifically for 50 nodes/cell. Figure 7 shows the simulation results of the CDF of the system capacity for downlink scenario, when the number of available bands is 9. It is observed in Fig. 7 that in case of downlink transmission, the median of the system capacity is 2.5 times that

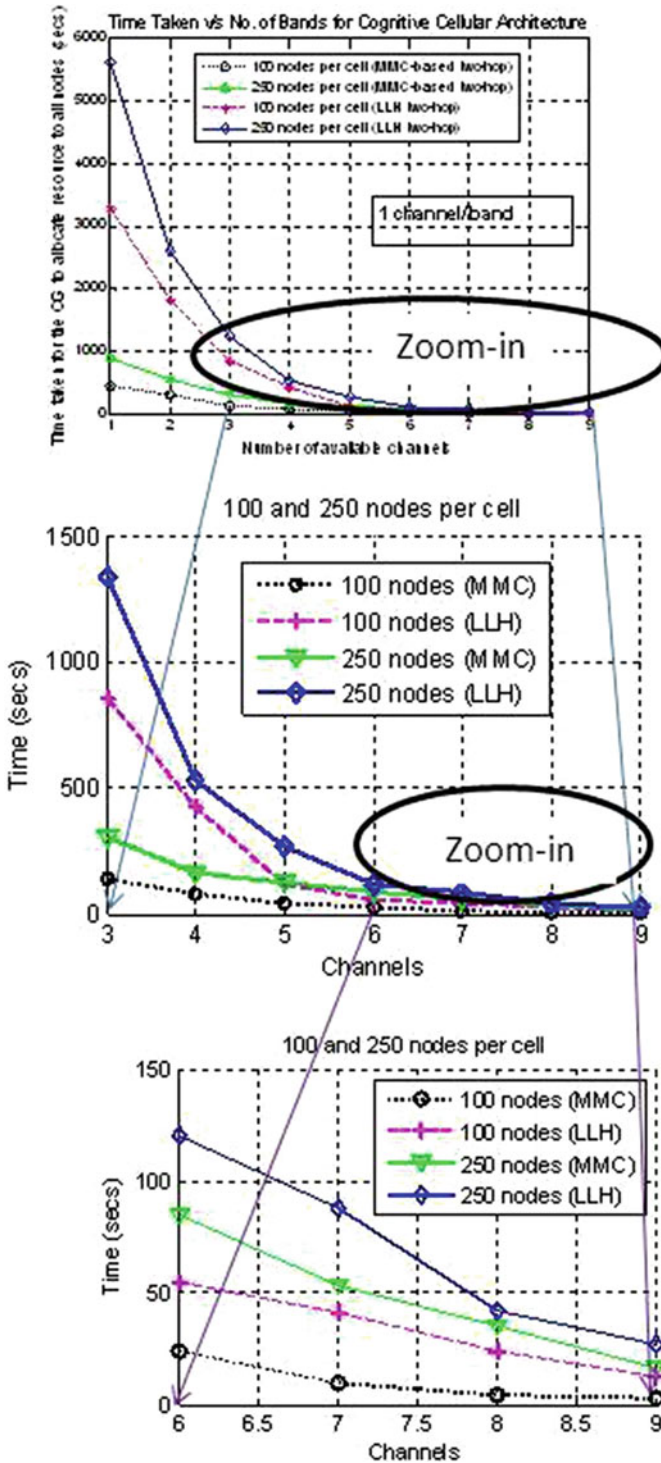


Fig. 5 Variation of time delay with number of frequency bands (100+ nodes per cell)

Table 1 Variation of time delay with number of frequency bands for different number of communication nodes

Nodes	Channels								
	1	2	3	4	5	6	7	8	9
20									
MMI	90	61	30	8	5	3.78	1.98	0.78	0.34
LLH	200	124	82	54	32	24	19	14	11
50									
MMI	172	98	51	32	16	9	6	4	3
LLH	493	354	206	183	123	89	62	43	22
100									
MMI	385	312	143	121	86	23	16	12	7
LLH	3054	1924	828	452	186	54	38	26	16
250									
MMI	950	523	327	234	165	86	52	34	21
LLH	5524	2723	1356	509	272	132	88	42	32

obtained from the single-hop network with no relay as CG, i.e., 150% improvement over the single-hop network. Similarly, the median value (0.5 value in CDF) of the MMI design is 2.8 bps/Hz/cell, which is more than twice obtained from the single-hop network value of 1.12 bps/Hz/cell. Significantly, the median of the system capacity of the MMI design is superior by 0.55 bps/Hz/cell to the LLH based method, whose expected value of the system capacity is 2.2 bps/Hz/cell; i.e., an improvement of 20% in the expected system capacity over LLH method. From Fig. 7, it can be observed that the maximum difference in the system capacity between MMI and LLH is reflected when the CDF is 0.1. At this point, the MMI has a system capacity of 2.1 bps/Hz/cell while the LLH has a system capacity of 1.1 bps/Hz/cell; thereby showing an improvement of 41%. The significant improvement in the system capacity observed in the MMI design for 50 nodes in the network—up to 150% improvement over single-hop and up to 40% over the state-of-the-art LLH method is due to the synchronized resource reuse scheme achievable through six dedicated CGs. On the other hand, in both the single-hop and the LLH method, there is no such scheme for effective reuse of spectrum resources.

5.3 Effect of Shadowing on the Optimum Position of CGs

In a real-world, the wireless channel results in significant distortion in the signal. In order to consider the effect of this distortion on the signal strength and the overall communication, a slow-fading channel is considered, wherein the random variation in the signal strength and thereby, the received power is accounted for by considering a log-normal shadowing across each path. Though empirical, this is a highly accurate mechanism to model channel fluctuations. A log-normal shadowing with zero mean and a standard deviation, varying from 2 to 6 dB is considered in this work. Further, in order to evaluate the system performance in the presence of shadowing, the shadowing distance (additional distance due to shadowing) is first calculated from the instantaneous shadowing value and substituted in Eq. (4) in order to find the value of φ that would maximize the value of γ . To begin with, the equation for γ given in (4) can be expanded to:

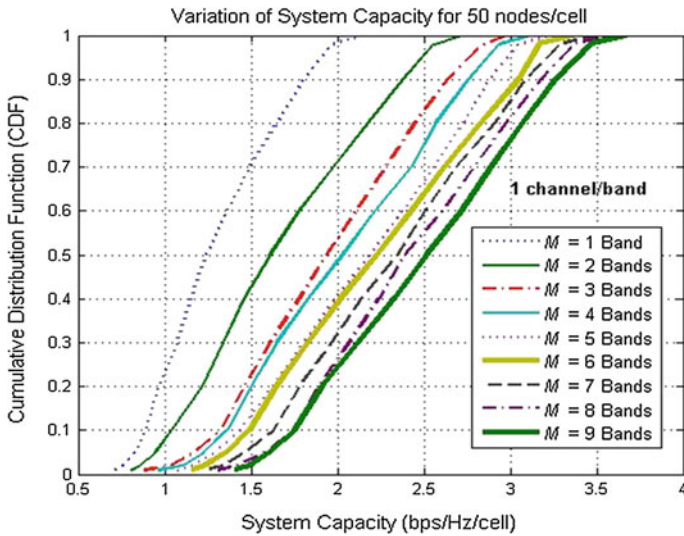


Fig. 6 Variation of system capacity for 50 nodes/cell

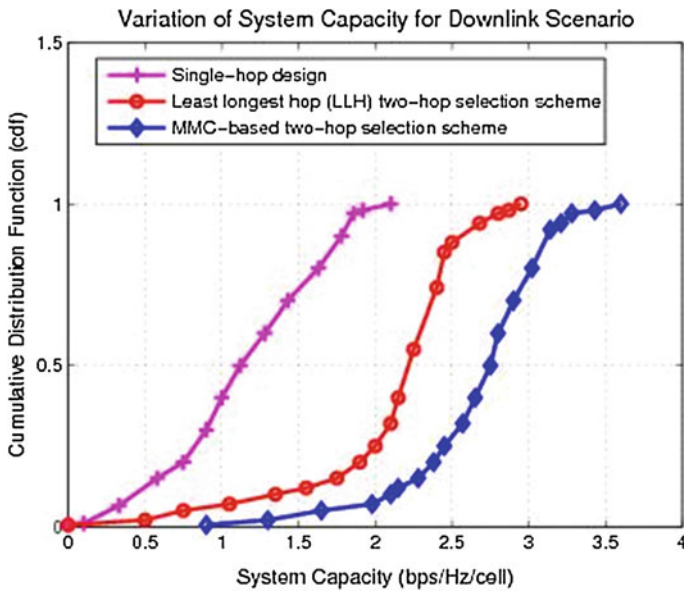


Fig. 7 Cumulative distribution function (CDF) of system capacity in the downlink of a multi-cellular network for nine bands when there are 50 nodes in the network

$$\gamma = (r/2 \times 10^{0.1\zeta_c})^{-\alpha} / \left(\sum_{i=1}^{n_t-1} \left(\left(\sqrt{((1.732r \cos \theta_i - \tau r \cos \varphi)^2 + (1.732r \sin \theta_i - \tau r \sin \varphi)^2)} \right) \times (10^{0.1\zeta_{int i}}) \right)^{-\alpha} \right) \tag{9}$$

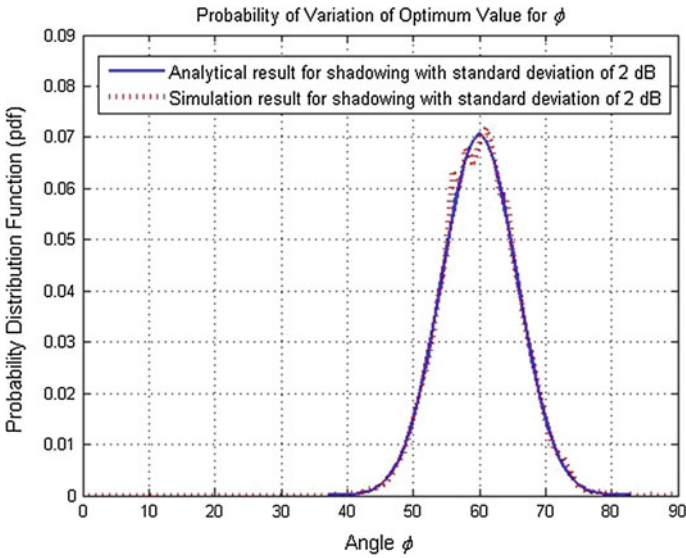


Fig. 8 Variation in the optimum position of CGs for low value of log-normal shadowing

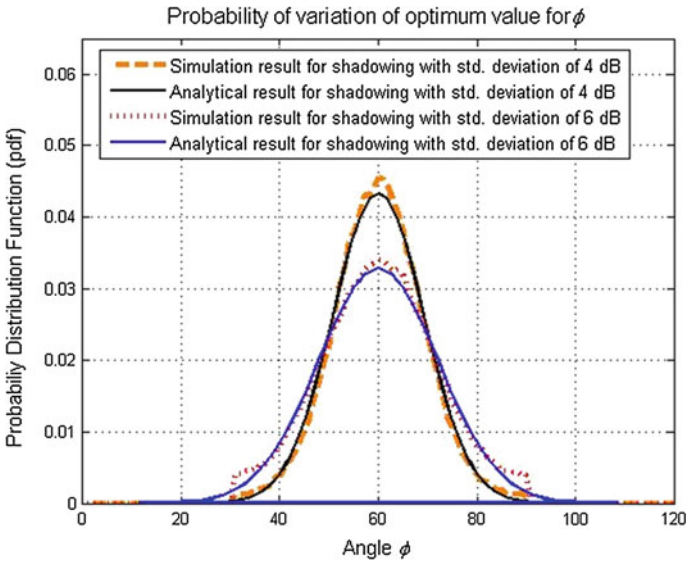


Fig. 9 Variation in the optimum position of CGs for mid-range value of log-normal shadowing

where, $\theta_i = (i - 1) \times 60 + 30$. Further, the simulation model assumes that the CGs are placed at half the distance between the BS and the edges of the cell. Hence, $\tau = 0.5$. The number of simultaneously communicating pairs in the 19-cell network is $n_t = 38$. Also with a coverage area of 10 Sq. km, $r = 62.04$ m. Different values of φ are then selected and the value of γ is then computed for each individual values of the standard deviation (2, 4, 6 and 8 dB).

Figures 8 and 9 show the results of optimum value of φ where the gateway should be placed that would maximize γ . These results were obtained by performing Monte Carlo

Table 2 Comparison of analytical and simulation results for different log-normal shadowing in wireless channel

Sr. No.	2 dB		4 dB		6 dB	
	Analytical	Simulation	Analytical	Simulation	Analytical	Simulation
Mean	60	59.92	60	60.05	60	60.18
SD	5.65	5.655	9.207	9.313	14.14	12.59

Table 3 Results of t tests for different values of log-normal shadowing

Parameters	2 dB	4 dB	6 dB
α	0.05	0.05	0.05
p value	0.9857	0.994	0.828
t-Stat	0.01797	0.00705	0.217
t-Critical	1.991	1.996	1.9902

simulations with 10,000 runs and calculating the average over these runs. It can be observed from Fig. 8 that when the standard deviation of log-normal shadowing for all the desired and the interfering transmissions is low (≤ 2 dB), the probability density function (PDF) of the optimum position of CG deviates only marginally from its initial value of $\pi/3$. The results show that the analytical and simulated values of standard deviation of φ for 2 dB variation in standard deviation of log-normal shadowing are 5.65 and 5.655 degrees, respectively. Significantly, Fig. 9 shows that with an increase in the standard deviation (≤ 6 dB), the PDF of the optimum location (where γ is maximized) deviates considerably. In fact, for 6 dB standard deviation, the optimum position of CG shifts by more than 30 degrees (beyond $\pi/6$ and $\pi/2$ on either side) with a non-zero probability. Notably, for a log-normal shadowing with a standard deviation of 4 dB, the analytical and simulated results in the standard deviation of φ are 9.207 and 9.313 while for a lognormal shadowing with a standard deviation of 6 dB, the analytical and simulated results in the standard deviation of φ are 14.14 and 12.59. This shows that there is a very close match in the standard deviation between the analytical model and the simulation results. Further, as can be observed in Table 2, for all three cases of log-normal shadowing (2, 4 and 6 dB), the simulation results point out that the mean remains nearly the same. Notably, in order to test the correctness of the analytical model, a statistical analysis based on t test has been carried out. With the optimum value for φ , for each considered scenario, the t tests compare the two sets of data assuming equal standard deviation and therefore equal variances. The t -tests results are also presented in Table 3. As noticed, in all three cases, the test statistic (t-Stat) $<$ critical value (t-Critical) and the p value $>$ significant level for all 2, 4 and 6 dB. Hence, the null hypothesis is accepted and thereby demonstrated that there is no statistical difference between the results provided by the analytical model and the simulation results. Importantly, this finding is stated with a very high level of confidence of 95% (significant level, $\alpha = 0.05$). However, it should be noted that as the shadowing increases (say, beyond 6 dB), the overall amount of interference also increases. This in turn implies that the interference from the second tier of cells (24 interferers from 12 cells in the second tier) play a significant role in the overall interference and the system quality. This requires further analysis/distance calculation from the second tier of cells and is not considered in this work. Finally, it should be noted that the placement of CG in non-optimum positions does not affect the basic premise of the multi-hop multi-band architecture. The MMI architecture would still function as described, albeit with reduced network capacity.

6 Conclusions and Future Work

In this paper a new multi-hop multi-band intelligent (MMI) architecture is proposed for next generation cellular networks. Under this design, a primary/secondary node is defined for spectrum resource allocation. When the primary user changes its state from passive to active mode, one or more gateways could change their transmission/reception band accordingly. But the frequency of the entire end-to-end communication link need not be changed. This results in a simple solution for frequency switching and resource allocation problem, especially in case of asymmetric traffic in cellular networks. In addition, due to the multi-hop architecture and multi-band model, a cognitive gateway needs to transmit only to its neighbouring gateways/mobile terminal. Significantly, MMI results in around 150% improvement in the system capacity of the cellular network, while at the same time, exponentially reducing the time taken for the allocation of frequency bands, as compared to single-hop and state-of-the-art based two-hop methods. The future research in the MMI design would be to determine the mechanism for feedback and exchange of signalling information.

Acknowledgments The authors would like to thank Enterprise Ireland (EI) for their graceful support. In addition, the authors would like to acknowledge Dr. Gabriel-Miro Muntean from Dublin City University (DCU), Ireland, Dr. Sinan Sinanovic and Prof. Harald Haas from the University of Edinburgh, UK for their input during the initial stages of this research.

References

1. Muntean, G. M., & Cranley, N. (2007). Resource efficient quality-oriented wireless broadcasting of adaptive multimedia content. *IEEE Transactions on Broadcasting*, 53(1), 362–368.
2. Ekstrom, H., et al. (2006). Technical solutions for the 3G long-term evolution. *IEEE Communication Magazine*, 44, 38–45.
3. Haykin, S. (2005). Cognitive radio: Brain-empowered wireless communications. *IEEE Journal on Selected Areas in Communication*, 23(2), 201–220.
4. Federal Communications Commission. (2002). *Spectrum policy task force*. Technical report, Docket No. 02–135, November 2002.
5. Arslan, H., & Celebi, H. (2007). *Software defined radio architectures for cognitive radios. Cognitive radio, software defined radio and adaptive wireless systems*. Berlin: Springer.
6. Mitola, J. (2000). Cognitive radio: An integrated agent architecture for software defined radio. Ph.D. dissertation, Royal Institute of Technology (KTH), Sockholm, Sweden, May 2000.
7. Venkataraman, H., & Muntean, G. M. (Eds.). (2012). *Cognitive radio and its application for next generation cellular networks*. Berlin: Springer.
8. Byungchan, A., Hyunsoo, Y., & Wan, C. J. (2001). A design of macro-micro CDMA cellular overlays in the existing big urban areas. *IEEE Journal on Selected Areas in Communications*, 19(10), 2094–2104.
9. Alyes, H., D'Souza, R., Fraidenraich, G., & Pellenz, M. E. (2012). *Throughput performance of parallel and repetition coding in incremental decode-and-forward relaying*. ACM Springer Wireless Networks (2012). doi:10.1007/s11276-012-0440-5.
10. Cabric, D., Mishra, S. M., & Brodersen, R. W. (2004). Implementation issues in spectrum sensing for cognitive radios. In *Asilomar conference on signals, systems and computers*.
11. Huang, X., Han, N., Zheng, G., Sohn, S., & Kim, J. (2007). Weighted collaborative spectrum sensing in cognitive radio. In *2nd International conference on communications and networking in China*, CHINA-COM, 22–24 August 2007.
12. Lee, J. K., Yoon, J. H., & Kim, J. U. (2007). A new spectral correlation approach to spectrum sensing for 802.22 WRAN system. In *International conference on intelligent pervasive computing*.
13. Wild, B., & Ramchandran, K. (2005). Detecting primary receivers for cognitive radio applications. In *New frontiers in dynamic spectrum access networks*, IEEE DySPAN
14. Kim, N.M., & et al. (2008). Robust cognitive radio based OFDM architecture with adaptive traffic allocation in time and frequency. *Electronics and Telecommunications Research Institute (ETRI) Journal*, 30(1), 21–32.

15. Arslan, H., Mahmoud, H. A., & Yucek, T. (2007). OFDM for cognitive radio: Merits and challenges. In *Cognitive radio, software defined radio and adaptive wireless systems*, Vol. XVIII. Springer. ISBN: 978-1-4020-5541-6.
16. Michalke, C., Venkataraman, H., Sinha, V., Rave, W., & Fettweis, G. (2005). Application of SQRD algorithm for MIMO OFDM systems. In *European wireless conference*, Cyprus.
17. Venkataraman, H., Michalke, C., Sinha, V., Rave, W., & Fettweis, G. (2004). An improved detection technique for receiver-oriented MIMO-OFDM systems. In *9th international OFDM workshop*, Dresden, Germany, 12–14 September, 2004.
18. Weiss, T., & Jondral, F. (2004). Spectrum pooling: An innovative strategy for the enhancement of spectrum efficiency. *IEEE Personal Communications*, 6(4), 13–18.
19. Attar, A., Nakhai, M. R., & Aghvami, A. H. (2008). Cognitive radio transmission based on direct sequence MC-CDMA. *IEEE Transactions on Wireless Communications*, 7(4), 1157–1162.
20. Niyato, D., & Hossain, E. (2008). Market-equilibrium, competitive and cooperative pricing for spectrum sharing in cognitive radio networks: Analysis and comparison. *IEEE Transactions on Wireless Communications*, 7(11), 4273–4283.
21. Wu, H., Qao, C., De, S., & Tonguz, O. (2001). Integrated cellular and adhoc relaying systems. *IEEE Journal on Selected Areas in Communication*, 19(10), 2105–2115.
22. Venkataraman, H., Haas, H., Yun, S., Lee, Y., & McLaughlin, S. (2005). Performance analysis of hybrid wireless networks. In *Proceedings of IEEE international symposium on personal indoor and mobile radio communications (PIMRC'05)*, Berlin, Germany, Vol. 3, pp. 1742–1746, September 2005.
23. Ananthapadmanabha, R., Manoj, B. S., & Murthy, C. S. R. (2001). Multihop cellular networks: The architecture and routing protocol. In *Proceedings of IEEE international symposium on personal indoor mobile radio communications*, Vol. 2. San Diego, USA.
24. Venkataraman, H., & Muntean, G. M. (2011). Dynamic time slot partitioning for multimedia transmission in two-hop cellular networks. *IEEE Transactions on Mobile Computing*, 10(4), 532–543.
25. Le, L., & Hossain, E. (2007). Multihop cellular networks: Potential gains, research challenges, and a resource allocation framework. *IEEE Communications Magazine*, 45, 66–73.
26. Venkataraman, H., Sinanovic, S., & Haas, H. (2008). Cluster-based design for two-hop cellular networks. *International Journal for Communications, Networks and Systems (IJCNS)*, 1(4), 370–385.
27. Ikki, S. S., & Ahmed, M. H. (2010). Performance analysis of best-path selection scheme for multi-hop amplify-and-forward relaying. *European Transaction on Telecommunications*, 21(7), 603–610.
28. Ann, S., & Kim, H. S. (2010). Relay association method for optimal path in IEEE 802.16j mobile multi-hop relay networks. *European Transaction on Telecommunications*, 21(6), 624–631.
29. Huang, J. H., Wang, L. C., Chang, C. J., & Su, W. S. (2010). Design of optimum relay location in two-hop cellular systems. *ACM/Springer Wireless Networks*, 16(8), 2179–2189.
30. Xie, R., Richard Yu, F., & Ji, H. (2011). Joint power allocation and beamforming with users selection for CR networks via discrete stochastic optimization. *ACM Wireless Networks*. doi:10.1007/s11276-012-0413-8.
31. Bian, K., & Park, J. M. (2006). MAC-layer misbehaviours in multi-hop cognitive radio networks. In *International conference on science, technology, and entrepreneurship (UKC)*, Korea, August 2006.
32. Shin, J., Lee, D. K., & Cho, H. S. (2009). Is a multi-hop relay scheme gainful in an IEEE 802.22-based cognitive radio system. *IEICE Transactions on Communications*, 92, 3528–3532.
33. Lin, Y. S., Liu, C. C., Li, K. M., & Chen, C. H. (2004). Design of an LTCC tri-band transceiver module for GPRS mobile applications. *IEEE Transactions on Microwave Theory and Techniques*, 52(12), 2097–2103.
34. Tzortzakakis, M., & Langley, R. J. (2007). Quad-band internal mobile phone antenna. *IEEE Transactions on Antennas and Propagation*, 55(7), 2097–2103.
35. Tchamov, N. T., Broussev, S. S., Uzunov, I. S., & Rantala, K. K. (2007). Dual-band LC VCO architecture with a fourth-order resonator. *IEEE Transactions on Circuits and Systems II: Express Briefs*, 54(3), 277–281.
36. Venkataraman, H., Jaini, P. K., & Revanth, S. (2009). Optimum position of relay stations for cluster-based two-hop cellular networks. *International Journal for Communications, Networks and Systems (IJCNS)*, 2(4), 283–292.
37. Venkataraman, H., Nainwal, S., & Shrivastava, P. (2010). Optimum number of gateways in cluster-based two-hop cellular networks. *AEU Journal, Science Direct*, 64(4), 310–321.
38. 3rd Generation Partnership Project (3GPP). Technical specification group radio access network. In *Selection procedures for the choice of radio transmission technologies of UMTS*. 3GPP TR 30.03U, May 1998. Retrieved November 30, 2006, from <http://www.3gpp.org/ftp/Specs/html-info/3003U.htm>.
39. Philips, C., Raine, S., Curtis, J., Bartels, S., Sicker, D., Grunwald, D., & McGregor, T. (2011). The efficacy of path loss models for fixed wireless links. In: *Proceedings of 12th ACM international conference on passive and active measurement (PAM)*, pp. 42–51.

40. Sreng, V., Yanikomeroglu, H., & Falconer, D. D. (2003). Relay selection strategies in cellular networks with peer-to-peer relaying. In *Proceedings of IEEE vehicular technology conference (VTC Fall'03)*, Orlando, Florida, USA, 6–9 October 2003.

Author Biographies



Dr. Hrishikesh Venkataraman did his Bachelors from Mumbai University in 2001, his Masters in Technology (M.Tech) from Indian Institute of Technology (IIT) Kanpur in 2004 and his Ph.D. from Jacobs University Bremen, Germany in 2007. He is currently a Research Fellow with the Irish national research centre—The RINCE Institute (Research Institute for Networks and Communications Engineering) located in Dublin City University (DCU), Ireland. Over the last 4 years, he has collaborated with different industries like Ericsson, Everseen and Educational Initiative Private Limited. He has received nearly 130 K Euros as PI/Collaborator and is a co-Investigator of DCU-IIT Delhi Indo-Irish initiative. Further, he has published more than 40 international publications, is an Executive Editor of Transactions on Emerging Telecommunication Technologies (ETT) and is a founding chair of Dublin ACM SIGMOBILE chapter.



Mr. Dipesh Gandhi did his Bachelors in Engineering in Information and Communication Technology (ICT) from Dhirubhai Ambani Institute for Information and Communication Technology (DAIICT), Gandhinagar, India in 2008. Subsequently, he has been working as R&D Engineer with MindTree Consultants Limited and is currently employed as Senior Engineer in ST Microelectronics, National Capital Region (NCR), Delhi.



Mr. Vikrant Tomar did his Bachelors in Engineering in Information and Communication Technology (ICT) from Dhirubhai Ambani Institute for Information and Communication Technology (DAIICT), Gandhinagar, India in 2008. He worked as Research Associate for 1 year in Indian Institute of Technology (IIT) Bombay; and currently pursuing his PhD in Telecom and Signal Processing Laboratory, McGill University, Montreal, QC, Canada.